Unified View of the Interaction of Tetrakis(carboxylato)dirhodium(II) with Axial Donor−Acceptor Ligands

Dirk V. Deubel*

Institute of Biomedical Sciences, IBMS, Academia Sinica, Taipei 11529, Taiwan, Republic of China, and Swiss Center for Scientific Computing, CSCS, Swiss Federal Institute of Technology, ETH Zurich, CH-6928 Manno, Switzerland[1]

Received April 11, 2002

Summary: Density functional calculations rationalize the bonding in [Rh$_2$*(μ-O*$_2$*CR)*$_4$*L] complexes with strong and very weak axial donor−acceptor ligands L such as "Arduengo" carbenes and aromatic hydrocarbons.*

Tetrakis(carboxylato)dirhodium(II) complexes, [$Rh_2(\mu$-$O_2CR)_4$], and related species are versatile compounds being currently used as catalysts,[2,3] anticancer agents,[4,5] and building blocks for supramolecular assemblies.[6−8] Recent experimental work has focused on the synthesis of complexes of [$Rh_2(\mu$-$O_2CR)_4$] with axial carbene ligands and their application to catalytic C−C formation reactions.[3] One- and two-dimensional networks consisting of [$Rh_2(\mu$-$O_2CCF_3)_4$] and polycyclic aromatic hydrocarbons (PAH) have been designed as well.[6] The PAH of these networks usually bind in an η^2 fashion at the axial positions.[6]

Despite a considerable interest in the electronic structure of Rh−Rh clusters of the type [$Rh_2(\mu$-$O_2CR)_4$][9,10] and of transition-metal carbene complexes,[11] the nature of the interaction in the novel complexes with axial ligands has not been understood entirely. The Rh−L bond strength in complexes with ligands such as carbenes and aromatic hydrocarbons is anticipated to be very different, and gaining a unified view of the bonding in these intriguing organometallic compounds is a major challenge. The objective of this density functional study[12] is to predict and to analyze[18−24] the metal−ligand bond energies in the model complexes [$Rh_2(\mu$-$O_2CH)_4$L] (**1a**−**d**) with the ligands L = CH_2 (**a**), imidazole 2-ylidene[25] (**b**), C_2H_4 (**c**), η^2-benzene (**d**). Calculated molecular geometries of [$Rh_2(\mu$-$O_2CH)_4$L] are presented in Figure 1;[26] the results of the energy analysis of the Rh−L bond are given in Table 1. We draw the following conclusions.

(i) Upon coordination of an axial ligand, **a**−**d**, the [$Rh_2(\mu$-$O_2CH)_4$L] core remains intact (Figure 1). The Rh−Rh bond is slightly elongated in **1a**−**d** (2.41−2.48 Å) in comparison to that in the parent dimer, **0** (2.38

* To whom correspondence should be addressed.

(1) URL: http://staff-www.uni-marburg.de/~deubel.

(2) Doyle, M. P.; Forbes, D. C. *Chem. Rev.* **1997**, *97*, 911 and references cited therein.

(3) (a) Padwa, A.; Snyder, J. P.; Curtis, E. A.; Sheehan, S. M.; Worsencroft, K. J.; Kappe, C. O. *J. Am. Chem. Soc.* **2000**, *122*, 8155. (b) Snyder, J. P.; Padwa, A.; Stengel, T.; Arduengo, A. J., III; Jockisch, A.; Kim, H.-J. *J. Am. Chem. Soc.* **2001**, *123*, 1131 and references cited therein.

(4) (a) Asara, J. M.; Hess, J. S.; Lozada, E.; Dunbar, K. R.; Allison, J. *J. Am. Chem. Soc.* **2000**, *122*, 8. (b) Sorasaenee, K.; Galán-Mascarós, J. R.; Dunbar, K. R. *Inorg. Chem.* **2002**, *41*, 433.

(5) (a) Clarke, M. J.; Zhu, F.; Frasca, D. R. *Chem. Rev.* **1999**, *99*, 2511. (b) Sadler, P. *Angew. Chem., Int. Ed.* **1999**, *38*, 1512.

(6) (a) Cotton, F. A.; Dikarev, E. V.; Stiriba, S.-E. *Organometallics* **1999**, *18*, 2724. (b) Cotton, F. A.; Dikarev, E. V.; Petrukhina, M. A. *J. Am. Chem. Soc.* **2001**, *123*, 11655 and references cited therein.

(7) Cotton, F. A.; Hillard, E. A.; Murillo, C. A. *J. Am. Chem. Soc.* **2002**, *124*, 5658.

(8) Miyasaka, H.; Campos-Fernandez, C. S.; Clerac, R.; Dunbar, K. R. *Angew. Chem., Int. Ed.* **2000**, *21*, 2831.

(9) (a) Cotton, F. A.; Feng, X. *J. Am. Chem. Soc.* **1998**, *120*, 3387. (b) Rodriguez-Garcia, C.; Gonzales-Blanco, O.; Oliva, A.; Ortuno, R. M.; Branchadell, V. *Eur. J. Inorg. Chem.* **2000**, 1073.

(10) Lichtenberger, D. L.; Pollard, J. R.; Lynn, M. A.; Cotton, F. A.; Feng, X. *J. Am. Chem. Soc.* **2000**, *122*, 3182.

(11) Selected references: (a) Cundari, T. R.; Gordon, M. S. *J. Am. Chem. Soc.* **1991**, *113*, 5231. (b) Jacobsen, H.; Ziegler, T. *Inorg. Chem.* **1996**, *35*, 775. (c) Vyboishchikov, S. F.; Frenking, G. *Chem. Eur. J.* **1998**, *4*, 1428. (d) Boehme, C.; Frenking, G. *Organometallics* **1998**, *17*, 5801. (e) Dalmazio, I.; Duante, H. A. *J. Chem. Phys.* **2001**, *115*, 1747.

(12) Geometry optimizations were performed at the gradient-corrected density-functional-theory (DFT) level using Becke's exchange functional and Perdew's correlation functional (BP86[13]). Relativistic effects were considered by the zeroth-order regular approximation (ZORA[14]). Uncontracted Slater-type orbitals (STOs) were used as basis functions.[15] The valence basis functions at the metal have triple-ζ quality, augmented with a set of p functions and a set of f functions. The valence basis set at the other atoms has triple-ζ quality, augmented with a set of d functions (VTZP). The $(1s)^2$ core electrons of C, N, and O and the $(1s2s2p3s3p3d)^{28}$ core electrons of Rh were treated within the frozen-core approximation.[16] The calculations were carried out with the ADF 2000 program package[17] using standard basis sets. The Rh−L interactions were analyzed using Ziegler and Rauk's energy decomposition scheme.[18−23]

(13) (a) Becke, A. D. *Phys. Rev. A* **1988**, *38*, 3098. (b) Perdew, J. P. *Phys. Rev. B* **1986**, *33*, 8822.

(14) Van Lenthe, E.; Ehlers, A. E.; Baerends, E. J. *J. Chem. Phys.* **1999**, *110*, 8943 and references cited therein.

(15) Snijders, J. G.; Baerends, E. J.; Vernooijs, P. *At. Data Nucl. Tables* **1982**, *26*, 483.

(16) Baerends, E. J.; Ellis, D. E.; Ros, P. *Chem. Phys.* **1973**, *2*, 41.

(17) (a) Bickelhaupt, F. M.; Baerends, E. J. In *Reviews in Computational Chemistry*; Lipkowitz, K. B., Boyd, D. B., Eds.; VCH: New York, 2000; Vol. 15, p 1. (b) Te Velde, G.; Bickelhaupt, F. M.; Baerends, E. J.; Fonseca Guerra, C.; Van Gisbergen, S. J. A.; Snijders, J. G.; Ziegler, T. *J. Comput. Chem.* **2001**, *22*, 931.

(18) (a) Ziegler, T.; Rauk, A. *Theor. Chim. Acta* **1977**, *46*, 1. (b) Ziegler, T.; Rauk, A. *Inorg. Chem.* **1979**, *18*, 1558. (c) Ziegler, T.; Rauk, A. *Inorg. Chem.* **1979**, *18*, 1755.

(19) Frenking, G.; Fröhlich, N. *Chem. Rev.* **2000**, *100*, 717.

(20) For recent examples, see: (a) Uddin, J.; Frenking, G. *J. Am. Chem. Soc.* **2001**, *123*, 1683. (b) Cedeño, D. L.; Weitz, E. *J. Am. Chem. Soc.* **2001**, *123*, 12857. (c) Deubel, D. V. *J. Am. Chem. Soc.*, in press.

(21) Bickelhaupt, F. M.; DeKock, R. L.; Baerends, E. J. *J. Am. Chem. Soc.* **2002**, *124*, 1500.

(22) Deubel, D. V.; Ziegler, T. *Organometallics* **2002**, *21*, 1603.

(23) Deubel, D. V. *J. Am. Chem. Soc.* **2002**, *124*, 5834.

(24) An alternative decomposition scheme is charge decomposition analysis (CDA); for examples, see: (a) Deubel, D. V.; Frenking, G. *J. Am. Chem. Soc.* **1999**, *121*, 2021. (b) Deubel, D. V.; Sundermeyer, J.; Frenking, G. *J. Am. Chem. Soc.* **2000**, *122*, 10101. (c) Deubel, D. V.; Schlecht, S.; Frenking, G. *J. Am. Chem. Soc.* **2001**, *123*, 10085 and references cited therein.

(25) Arduengo, A. J., III; Harlow, R. L.; Kline, M. *J. Am. Chem. Soc.* **1991**, *113*, 361.

10.1021/om020285j CCC: $22.00
Publication on Web 09/19/2002

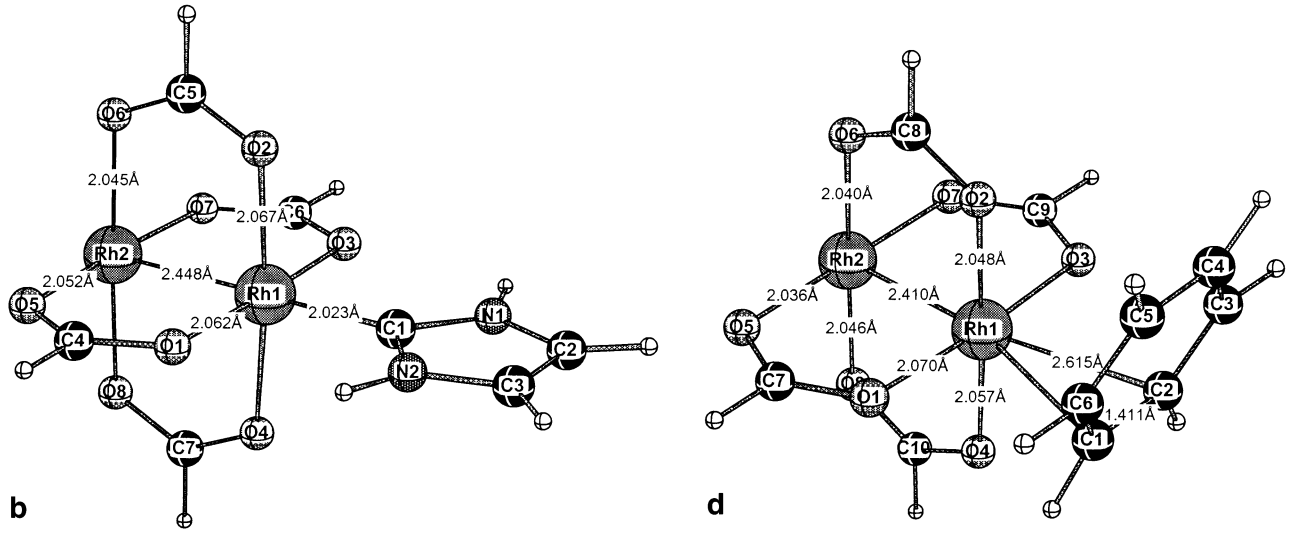

Figure 1. Calculated structures of $[Rh_2(O_2CH)_4L]$ (**1b**, C_{2v}; **1d**, C_s).

Table 1. Energy Decomposition of the Rh−L Bond in the C_{2v}-Symmetric Complexes $[Rh_2(O_2CH)_4L]$ (1a−d) (Energies in kcal/mol), Ratio of Electrostatics and Stabilizing Orbital Interactions ΔE_{elst}:ΔE_{orb}, and Ratio of σ and π Interactions $\Delta E_{orb}(\sigma)$:$\Delta E_{orb}(\pi)$

contribn	descripn	Γ_i	1a	1b	1c	1d[d]
ΔE_{prep}(L)	def of the ligand L		18.7[a]	1.0	2.3	0.7
ΔE_{prep}([Rh_2])	def of $[Rh_2(O_2CH)_4]$		2.3	1.7	2.2	0.9
ΔE_{prep}	prep energy of the fragments; $\Delta E_{prep} = \Delta E_{prep}(L) + \Delta E_{prep}([Rh_2])$		21.0	2.7	4.5	1.6
ΔE_{Pauli}	Pauli repulsion		281.9	192.3	112.3	43.0
ΔE_{elst}	electrostatic interactions		−229.1	−168.8	−79.9	−28.3
ΔE_{orb}	stabilizing orbital interactions		−131.5	−71.6	−53.6	−22.1
$\Delta E_{orb}(\Gamma_i)$	contribns from the irred	a_1	−70.6[b]	−55.2[b]	−28.5[b]	−15.9[b,e]
	representations, Γ_i, to ΔE_{orb};	a_2	0.0	−0.3	−0.7	
	$\Delta E_{orb} = \sum_i \Delta E(\Gamma_i)$	b_1	−54.2[c]	−10.6[c]	−2.6	
		b_2	−6.7	−5.6	−21.9[c]	−6.2[c,f]
ΔE_{int}	interaction energy; $\Delta E_{int} = \Delta E_{Pauli} + \Delta E_{elst} + \Delta E_{orb}$		−78.7	−48.1	−21.2	−7.4
ΔE	bond energy; $\Delta E = \Delta E_{prep} + \Delta E_{int}$		−57.7	−45.4	−17.0	−5.7
ΔE_{elst}:ΔE_{orb}	electrostatics vs orbital int		1.7	2.4	1.5	1.3
$\Delta E_{orb}(\sigma)$:$\Delta E_{orb}(\pi)$	σ versus π interactions		1.3	5.2	1.3	2.6

[a] Contains the $^3B_1 \rightarrow {}^1A_1$ excitation energy of methylene. [b] σ donation. [c] π back-donation. [d] C_s symmetry. [e] a′. [f] a″.

Å). The Rh−ligand distances are calculated to be 1.89 (**a**), 2.02 (**b**), 2.19 (**c**), and 2.52 Å (**d**).

(ii) A wide range of the Rh−L bond energies ΔE is predicted with values of −57.7 (**a**), −45.5 (**b**), −17.0 (**c**), and −5.7 kcal/mol (**d**) (Table 1). The trend in the bond energies in **1a**−**d** is evident from the calculated metal−ligand distances.

(iii) Deformation of the free molecules, $[Rh_2(\mu\text{-}O_2CH)_4]$ and L, toward their geometry in the complexes **1b**−**d** requires a small preparation energy, ΔE_{prep}, of less than 3 kcal/mol for each molecule (Table 1), whereas the ΔE_{prep} value for methylene also contains the $^3B_1 \rightarrow {}^1A_1$ excitation energy.[27] The energy of interaction, ΔE_{int}, between $[Rh_2(\mu\text{-}O_2CH)_4]$ and L is the main factor determining bond energy ($\Delta E = \Delta E_{prep} + \Delta E_{int}$). ΔE_{int} can in turn be divided into three parts ($\Delta E_{int} = \Delta E_{Pauli} + \Delta E_{elst} + \Delta E_{orb}$): Pauli repulsion, ΔE_{Pauli}, the electrostatic contribution, ΔE_{elst}, and the stabilizing orbital interactions, ΔE_{orb}. The analysis shows that $|\Delta E_{int}|$ and each of its three contributions decrease in the order **1a** > **1b** > **1c** > **1d** (Table 1).

(iv) Electrostatic interactions (ΔE_{elst}) cause a stronger stabilization of the Rh−L bond in **1a**−**d** than orbital interactions (ΔE_{orb}). The ratio ΔE_{elst}:ΔE_{orb} is predicted to be 1.7 (**a**), 2.4 (**b**), 1.5 (**c**), and 1.3 (**d**) (Table 1), indicating that electrostatic attraction is particularly important in the carbene complexes.

(v) Given the small value of Pauli repulsion[21] in the η^2-benzene complex **1d** in comparison with ΔE_{Pauli} in the other complexes, one might believe that Pauli repulsion is least important in **1d** (Table 1). One should note that the Rh−C distances in the benzene complex are much longer[28] than in the ethylene complex **1c** and that the benzene moiety is bent away from the carboxylato ligands (Figure 1). The equilibrium structure of **1d** is the *result* of Pauli repulsion between oxygen lone pairs and the π-electron system. Analysis of the ethylene complex $[Rh_2(\mu\text{-}O_2CH)_4(C_2H_4)]$ (**1c′**) with Rh−C bond lengths taken from the optimized structure of **1d** reveals virtually equal amounts of Pauli repulsion in **1c′** and

(26) Calculated bond distances and valence angles in the complexes $[Rh_2(\mu\text{-}O_2CH)_4L_n]$ with $n = 0$ (**0**), $n = 1$ (**1a**−**d**), and $n = 2$ (**2a**−**c**) are listed in the Supporting Information. The calculated structures show D_{4h} (**0**), C_{2v} (**1a**−**c**), C_{2v} (**1d**), and D_{2d} symmetry (**2a**−**c**); these structures were also obtained by geometry optimizations using selected starting structures of lower symmetry.

(27) Note that the calculated $^3B_1$−$^1A_1$ singlet−triplet splitting of methylene at the BP86 level (15.7 kcal/mol) is larger than the experimental value (9 kcal/mol): McKellar, A. R. W.; Buenker, P. R.; Sears, T. J.; Evenson, K. M.; Saykally, R. J.; Langhoff, S. R. *J. Chem. Phys.* **1983**, *79*, 5251.

(28) The long Rh−C distances (2.615 Å) in **1d** are similar to those (2.770 Å, 2.787 Å) in an X-ray crystal structure of $[Rh_2(\mu\text{-}O_2CCF_3)_4$-(hexamethylbenzene)]$_\infty$.[6a]

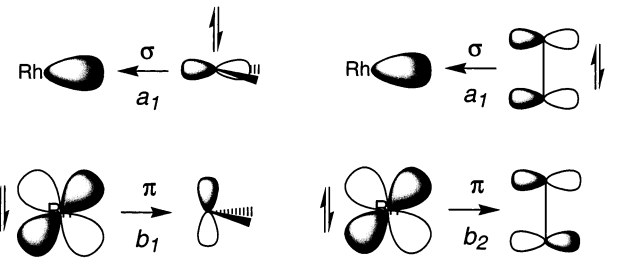

Figure 2. Schematic representation of σ donation and π back-donation between $[Rh_2(O_2CH)_4]$ and $^1A_1$ methylene (left) as well as between $[Rh_2(O_2CH)_4]$ and ethylene (right).

1d and a larger stabilization by electrostatics as well as by stabilizing orbital interactions in **1c′**, indicating a slight intrinsic preference of the metal for the olefin ligand (see Supporting Information).

(vi) Partitioning of the orbital-interaction term ΔE_{orb} into the irreducible representations Γ_i ($\Delta E_{orb} = \sum_i \Delta E(\Gamma_i)$) reveals the contributions from σ and π interactions to the bond energy; the predominant σ and π orbital interactions in metal−carbene and metal−ethylene bonds are displayed in Figure 2.[29] σ donation from occupied L orbitals into vacant $[Rh_2(\mu\text{-}O_2CH)_4]$ orbitals is represented by a_1 (in **1a**−**c**) and a' (in **1d**), respectively, while π back-donation from occupied $[Rh_2(\mu\text{-}O_2CH)_4]$ orbitals into vacant L orbitals is represented by b_1 (in **1a**,**b**), b_2 (in **1c**), and a'' (in **1d**), respectively (Table 1). The analysis shows that σ donation is slightly more important than π back-donation in the methylene and ethylene complexes **1a**,**c**; the ratio σ:π of the energies is 1.3 (Table 1). In contrast, in the complexes of both the heterocyclic carbene and benzene, π back-donation is much weaker; the analysis predicts the ratio σ:π of 5.2 in **1b** and 2.6 in **1d**. Inspection of the atomic partial charges shows that the central carbon (here denoted C1) in free imidazol-2-ylidene is negatively charged (−0.19; see the Supporting Information), which is due to electron redistribution into the p_z orbital of C1 within the aromatic π system of the free heterocycle. This orbital can only partially act as an acceptor orbital for electron back-donation from the metal in **1b**. In contrast, the long metal−ligand distance in the η^2-benzene complex induced by Pauli repulsion is the origin of the weak π back-donation in **1d**, because π interactions require shorter interatomic distances than σ interactions.[22,30]

(vii) Uptake of a second axial carbene or ethylene ligand leads to a significant stabilization and decreases the energy of the Rh−L bond by approximately only 20% in **2a**−**c** (Table 2), indicating that carbene complexes of the type $[Rh_2(\mu\text{-}O_2CH)_4L_2]$ should be considered interesting targets for synthesis and potential intermediates in the catalytic systems.[3] However, while the geometry of the dirhodium core in the $[Rh_2(\mu\text{-}O_2CH)_4L_2]$ complexes **2b**,**c** is almost unaffected by the second axial ligand, the dimethylene complex **2a** shows a very long Rh−Rh distance (2.87 Å).[31]

Current work on dirhodium carboxylates is aimed at an understanding of their anticancer activity.[4] We are presently analyzing the interaction of dirhodium(II) complexes with potential biological targets to compare the chemoselectivity of the metalation of biomolecules by the title compounds and by the antitumor drug cisplatin.[23]

Table 2. Calculated Energy per Rh−L Bond (in kcal/mol) in the Complexes $[Rh_2(O_2CH)_4L_n]$ (n = 1, 1a−d; n = 2, 2a−c)

n	a	b	c	d
1	−57.7	−45.4	−17.0	−5.8
2	−46.3	−33.9	−14.1	

Acknowledgment. I thank the Federal Ministry of Education and Research of Germany and the *Fonds der Chemischen Industrie* for a Liebig Fellowship.

Supporting Information Available: Tables giving calculated structural parameters of **0**, **1a**−**d**, and **2a**−**c**, Hirshfeld[32] atomic partial charges, and an analysis of the Rh−L bond energy in **1c′** and figures giving calculated molecular geometries of **0**, **1a,c**, and **2a**−**c**. This material is available free of charge via the Internet at http://pubs.acs.org.

OM020285J

(29) Figure 2 is based on the analysis of the orbital interactions in **1a** and **1c** in C_{2v} symmetry. Upon coordination of singlet methylene to $[Rh_2(\mu\text{-}O_2CH)_4]$ (complex **1a**), the population of the methylene HOMO (a_1) decreases by −0.75e and the population of the $[Rh_2(\mu\text{-}O_2CH)_4]$ LUMO (a_1) increases by 0.71e. The $[Rh_2(\mu\text{-}O_2CH)_4]$ LUMO (a_1) is a linear combination of the d_{z^2} orbitals of the two Rh centers (σ* orbital). The population of the methylene LUMO (b_1) increases by 0.63e and the population of the $[Rh_2(\mu\text{-}O_2CH)_4]$ HOMO-1 (b_1) decreases by −0.61e. The $[Rh_2(\mu\text{-}O_2CH)_4]$ HOMO-1 (b_1) is a linear combination of the d_{xz} orbitals of the two Rh centers (one of the π* orbitals). In the ethylene complex (**1c**), the population of the ethylene HOMO (a_1) decreases by −0.32e and the population of the $[Rh_2(\mu\text{-}O_2CH)_4]$ LUMO (a_1) increases by 0.28e. The population of the ethylene LUMO (b_2) increases by 0.22e, and the population of the $[Rh_2(\mu\text{-}O_2CH)_4]$ HOMO-1 (b_2) decreases by −0.16e. The $[Rh_2(\mu\text{-}O_2CH)_4]$ HOMO-1 (b_2) is a linear combination of the d_{yz} orbitals of the two Rh centers.

(30) (a) Deubel, D. V.; Frenking, G.; Senn, H. M.; Sundermeyer, J. *Chem. Commun.* **2000**, 2468. (b) Deubel, D. V. *J. Org. Chem.* **2001**, *66*, 3790.

(31) The structure of **2a** was also optimized at several DFT and ab initio levels of theory using Gaussian 98 (www.gaussian.com) with the SDD ECP and basis set, giving Rh−Rh distances of 2.864 Å (B3PW91), 2.918 Å (B3LYP), and 3.741 Å (MP2), respectively. These results clearly indicate that the metal−metal bond in the hypothetical dimethylene complex is strongly elongated, if not cleaved.

(32) Hirshfeld, E. L. *Theor. Chim. Acta* **1977**, *44*, 129.